Macromolecules ARTICLE

Macromolecules **2010**, *43*, 7101–7110 **7101**
DOI: 10.1021/ma1008572

Benzothiadiazole-Containing Pendant Polymers Prepared by RAFT and Their Electro-Optical Properties

Matthias Häussler,*,[†] Y. Phei Lok,[†] Ming Chen,[†] Jacek Jasieniak,[†] Raju Adhikari,[†] Simon P. King,[‡] Saif A. Haque,[‡] Craig M. Forsyth,[§] Kevin Winzenberg,[†] Scott E. Watkins,[†] Ezio Rizzardo,[†] and Gerard J. Wilson[†]

[†]*CSIRO Materials Science and Engineering, Bayview Avenue, Clayton, Vic 3168, Australia,* [‡]*Department of Chemistry, Imperial College London, London SW7 2AZ, United Kingdom, and* [§]*School of Chemistry, Monash University, Clayton, Vic 3800, Australia*

Received April 19, 2010; Revised Manuscript Received July 6, 2010

ABSTRACT: The synthesis of a series of novel, unsymmetrically substituted benzothiadiazole-containing vinyl monomers and their free radical polymerization with and without the control of a reversible addition−fragmentation chain transfer (RAFT) agent is reported. The resulting polymers with electroactive pendants show tunable absorption and emission spectra depending on their molecular architecture. Using RAFT allows the synthesis of block copolymers using a hole-transporting vinyl-triarylamine as a second monomer. Efficient energy transfer between the two pendants has been detected. Cyclic voltammetry and photoelectron spectroscopy in air measurements have been employed to reveal the location of the HOMO and LUMO of the block copolymers. The block copolymers also influence the morphology of spin-casted films and show rectifying behavior in organic photovoltaic devices.

Introduction

Plastic electronics is an emerging field of intense research, where high performing organic semiconductors have the potential to deliver low-cost solutions, particularly in areas such as thin-film transistors, organic light-emitting diodes (OLEDs), and organic photovoltaics.[1] For most of these devices, control of the morphology of the active layer is important in optimizing the device performance. For example, organic solar cells consist of a blend of donor and acceptor materials with the need for order on the nanoscale to compensate for the low exciton diffusion length of organic materials.[2] In most cases, a thermal annealing step after the blend deposition enables the donor and acceptor to assemble in a bicontinuous morphology. However, this desired morphology is often only metastable and far away from the thermodynamic minimum of complete phase-separation.[3]

Lamellar-type structures are postulated to be ideal for organic photovoltaic devices.[4] Block copolymers are known to self-assemble into various morphologies and also to stabilize blends between two immiscible materials by acting as a compatibilizer.[3c,5] Block copolymers are typically made by living polymerization, where the chain-ends of the first block can initiate or control the addition of the second block. Among all methods available, reversible addition−fragmentation chain transfer (RAFT) polymerization is one of the most versatile methodologies for controlling the architecture of a polymer chain and can be applied to a wide range of vinyl monomers.[6] The RAFT process equips a conventional radical polymerization with living characteristics through the presence of chain transfer agents such as thiocarbonylthio compounds S═C(Z)−SR. Such control enabled the synthesis of well-defined light-harvesting polymers, as previously demonstrated by our group.[7] Because of their pendant character and limited π−conjugation length, the polymers obtained in those studies, however, mainly absorbed in the UV range and have only limited use for applications such as organic photovoltaics. To date, only a few examples of side-chain-functionalized polymers have been reported, mainly using perylene diimide as chromophore.[8] This calls for the design of new monomers with lower bandgaps, allowing extended absorption into the visible region. One methodology could be to increase the π-conjugation length of the pendant monomer. Although very useful, this approach has its limitations as the molecular weights (MWs) of the monomers quickly become too large. Other methods include π-conjugated length alterations, increased aromaticity, substituent effects, and intermolecular interactions, which are often limited to fully conjugated polymer systems.[9] Another approach that provides a more feasible way of lowering the bandgap in pendant systems is the use of donor−acceptor (D−A) or partial charge-transfer chromophores. These donor−acceptor chromophores are formed when strong electron-donating and strong electron-withdrawing moieties interact through the high-lying HOMO of the donor and the low-lying LUMO of the acceptor.[10] The hybridization of these two orbitals results in new D−A orbitals with a smaller bandgap. Low bandgap materials reported in the literature are often based on electron-rich aromatic building blocks such as thiophenes or pyrroles sandwiching electron-poor *o*-quinoid units like benzothiadiazole (BT) or benzobisthiadiazole.[11]

In this contribution, we report the design and synthesis of new unsymmetrically substituted monomers containing the BT group as well as their radical polymerization with and without the control of a RAFT agent. Furthermore, the use of RAFT polymerization allows for the synthesis of block copolymers by using a vinyltriarylamine as the second monomer. We studied the thermal and optical properties of all of the new electroactive polymers as well as the morphology of spin-casted films. Finally, initial results for their use as the active layer in a bulk heterojunction solar cell will be reported.

Experimental Section

Materials. 4-Vinylphenylboronic acid, 4-methoxyphenylboronic acid, and 4-methylphenylboronic acid were purchased

*Corresponding author. E-mail: Matthias.Haeussler@csiro.au.

from Boron Molecular. 4-Bromo-2,1,3-benzothiadiazole, 4,7-dibromo-2,1,3-benzothiadiazole,[12] potassium vinyltrifluoroborate,[13] and 2-cyanopropan-2-yl butyl trithiocarbonate[14] were prepared according to literature methods. 2,2′-(Diazene-1,2-diyl)bis(2-methylpropanenitrile) (AIBN), 1,1′-(diazene-1,2-diyl)-dicyclohexanecarbonitrile (Vazo-88), and 1,2-bis(2,4,4-trimethylpentan-2-yl)diazene (V110) were obtained from TCI, Dupont, and Wako, respectively. Silica gel (0.040 to 0.063 mm) and thin layer chromatography plates (TLC silica gel 60 F_{254}) used for column chromatography were purchased from Merck. All other starting materials were obtained from Aldrich and were used as received. Solvents used for absorption and fluorescence measurements were spectroscopic grade, and solutions were degassed by nitrogen prior to spectroscopic measurements.

Methods. ^{1}H and ^{13}C NMR spectra were obtained on a Bruker AC-400 spectrometer in deuterated chloroform. UV−vis absorption spectra were recorded on a Cary 5E spectrophotometer. Steady-state fluorescence spectra were recorded on a Perkin-Elmer LS50 fluorimeter. The optical densities of the solutions for fluorescence measurements were kept below 0.15 at the excitation wavelength. We carried out time-correlated single photon counting experiments by employing a Jobin Yvon IBH fluorocube laser system. Excitation was performed at 467 nm (1 MHz, 80 μW cm^{-2} average intensity, instrument response 250 ps fwhm), and the emission was detected at 600 and 650 nm. Photoelectron spectroscopy in air (PESA) measurements were recorded with a Riken Keiki AC-2 PESA spectrometer with a power setting of 5−10 nW and a power number of 0.5. Samples for PESA were prepared on glass substrates. The electrochemistry measurements were carried out using a Powerlab ML160 potentiostat interfaced via a Powerlab 4/20 controller to a PC running Echem for Windows version 1.5.2. The measurements were run in argon-purged acetonitrile with tetrabutylammonium hexafluorophosphate (0.1 M) as the supporting electrolyte. The voltammograms were recorded using a standard three-electrode configuration with a glassy carbon (2 mm diameter) working electrode, a platinum wire counter electrode, and a silver wire pseudoreference electrode. The silver wire was cleaned in concentrated nitric acid and then in concentrated hydrochloric acid to generate the Ag/Ag^{+} reference. Voltammograms were recorded with a sweep rate of 50−200 mV s^{-1}. The sample concentration for monomers in solution was 1 mM. For the polymers, we prepared films of the polymers on the working electrode by drop-casting toluene solutions onto the working electrode. All potentials were referenced to the $E_{1/2}$ of the ferrocene/ferrocenium couple. The highest occupied molecular orbital (HOMO) and lowest unoccupied molecular orbital (LUMO) were estimated from the onsets of the oxidation and reduction peak, respectively, versus the midpoint potential of ferrocene, which was added as internal reference. MW data were obtained by gel permeation chromatography (GPC). Tetrahydrofuran (1.0 mL min^{-1}) was used as eluent. The GPC was calibrated with narrow polydispersity polystyrene (PS) standards, and MWs are reported as PS equivalents. Differential scanning calorimetry (DSC) analyses were conducted on a Mettler Toledo 821 apparatus with "Star Software" version 9. The module was calibrated with indium/zinc total method. Samples were run in alternating DSC mode with an underlying heating rate of 10 °C min^{-1}. Samples were encapsulated in lightweight aluminum pans. A sample size between 5 and 10 mg was used. Thermogravimetric analyses (TGA) were conducted on a Mettler Toledo TGA/STDA851 apparatus with "Star Software" version 9. Samples of ~10 mg were placed in a 70 μm alumina pan and run with a heating rate of 10 °C min^{-1} under nitrogen. Atomic force microscopy (AFM) images were recorded on a Pacific Nanotechnology microscope (Nano-R2).

Device Fabrication. ITO-coated glass (Kintek, 15 Ω/cm2) was cleaned by standing in a stirred solution of 5% (v/v) Deconex 12PA detergent at 90 °C for 20 min. The ITO was then successively sonicated for 10 min each in distilled water, acetone, and isopropanol. The substrates were then exposed to a UV-ozone clean (at RT) for 10 min. The PEDOT/PSS (HC Starck, Baytron P AI 4083) was filtered (0.2 μm RC filter) and deposited by spin coating at 5000 rpm for 60 s to give a 38 nm layer. The PEDOT/PSS layer was then annealed on a hot plate in the glovebox at 145 °C for 10 min. The polymers and PCBM (Nano-C) were dissolved in *o*-dichlorobenzene (Aldrich, anhydrous) in individual vials with stirring. The solutions were then combined, filtered (0.2 μm RC filter), and deposited by spin coating. The coated substrates were then transferred (without exposure to air) to a vacuum evaporator in an adjacent glovebox. A layer of Ca (20 nm) and then Al (100 nm) was deposited by thermal evaporation at pressures below 2×10^{-6} mbar. The total active device area was 0.2 cm^{2}. We made a connection point for the ITO electrode by manually scratching off a small area of the active layers. A small amount of silver paint (Silver Print II, GC electronics, part no. 22-023) was then deposited onto all of the connection points, both ITO and Al. The completed devices were then encapsulated with glass and a UV-cured epoxy (Summers Optical, lens bond type J-91) by exposing to 365 nm UV light inside a glovebox (H_2O and O_2 levels both < 1 ppm) for 10 min. The encapsulated devices were then removed from the glovebox and tested in air within 1 h. Electrical connections were made using alligator clips. The cells were tested with an Oriel solar simulator fitted with a 1000 W Xe lamp filtered to give an output of 100 mW/cm^{2} at AM 1.5. The lamp was calibrated using a standard, filtered Si cell from Peccell Limited, which was subsequently cross-calibrated with a standard reference cell traceable to the National Renewable Energy Laboratory. The devices were tested using a Keithley 2400 Sourcemeter controlled by Labview Software.

Synthesis of *N*,*N*-Di-*p*-tolyl-3-vinylaniline (2). A mixture of 3-bromostyrene (5 g, 27.3 mmol), di-*p*-tolylamine (**1**, 5.9 g, 30 mmol), sodium *tert*-butoxide (3.9 g, 41 mmol), bis(dibenzylideneacetone) palladium (0.157 g, 0.29 mmol), and tri-*tert*-butylphosphonium tetrafluoroborate 0.063 g (0.22 mmol) in 20 mL of anhydrous toluene was degassed and stirred under nitrogen overnight. Afterward, 50 mL of dichloromethane and 100 mL of 5% hydrochloric acid were added, and the solution was vigorously stirred for 30 min. The organic layer was separated, washed three times with 100 mL of water, and dried over $MgSO_4$. The product was further purified by column chromatography using 5% DCM in hexane, giving a white solid (7 g, 85%). ^{1}H NMR ($CDCl_3$, δ): 2.31 (s, 6H, CH_3), 5.62 5.19 (d, 1H, =CH*H*), (d, 1H, =C*H*H), 6.61 (dd, 1H, =CArH), 7.08−7.02 (m, 12H, ArH).

Synthesis of 4-(4-Bromo-phenyl)-2,1,3-benzothiadiazole. 4-Bromophenyl boronic acid (2.82 g, 13.1 mmol) and 4-bromo-2,1,3-benzothiadiazole (3.0 g, 14.9 mmol) were dissolved in toluene (40 mL) and THF (30 mL). A solution of Na_2CO_3 (2.36 g, 25.0 mmol) in water (16 mL) was added, followed by [$Pd(PPh_3)_4$] (1.6 g, 10 mol %). The reaction mixture was stirred vigorously while heating at reflux at 85 °C for 18 h. The reaction mixture was poured in iced water (400 mL), and this aqueous mixture was extracted with ether (3 × 250 mL). The combined ether extracts were dried ($MgSO_4$), filtered, and evaporated to dryness. A minimum volume of ethyl acetate was added to this crude product, and insoluble impurities were filtered. The filtrate was purified by column chromatography with petroleum ether 40−60 ($PETH_{40-60}$), followed by 20:80 DCM/$PETH_{40-60}$). Fractions were combined, evaporated to dryness, and recrystallized from ethyl acetate to give the product as bright-yellow needles. 2.56 g (63%). TLC (5% ethyl acetate/$PETH_{40-60}$) R_f = 0.30. mp 106.4−107.9 °C. ^{1}H NMR ($CDCl_3$, δ): 7.54−7.71 (m, 4H), 7.81−7.83 (m, 2H), 8.00−8.04 (m, 1H). ^{13}C NMR ($CDCl_3$): 121.0, 122.8, 127.6, 129.6, 130.8, 131.8, 133.3, 136.2, 153.2, 155.6. GC-MS (EI): *m*/*z* 292.0.

Synthesis of 4-(4-Vinylphenyl)-2,1,3-benzothiadiazole (4). Monomer **4** was prepared using the reaction conditions described by Molander and Rivero.[13] To a solution of 4-(4-Bromo-phenyl)-benzo-[1,2,5]thiadiazole (0.68 g, 2.3 mmol), potassium vinyltrifluoroborate

(0.447 g, 3.7 mmol), and [1,1-bis(diphenylphosphino)ferrocene]dichloropalladium(II) [$PdCl_2$(dppf)] in THF (25 mL) was added a solution of Cs_2CO_3 (2.3 g, 7.0 mmol) in water (4 mL). The reaction mixture was heated at reflux for 4 h. After the reaction mixture was quenched in iced water, the aqueous mixture was extracted with ether (4 × 150 mL). The combined organic extracts were washed with 20 wt % aqueous citric acid (3 × 200 mL), aqueous 1 M HCl (1 × 200 mL), and saturated brine (1 × 100 mL). This ether solution was then dried ($MgSO_4$), filtered, and the filtrate evaporated to dryness. The resulting residue was dissolved in DCM and filtered through a silica gel plug to give the product as a bright-yellow solid (0.44 g, 79%). TLC (5% ethyl acetate/PETH$_{40-60}$) R_f = 0.33. mp 56.9−59.6 °C. ^{1}H NMR ($CDCl_3$, δ): 5.32 (dd, 1H, =C*H*H), 5.85 (dd, 1H, =CH*H*), 7.57 (d, 2H, Ar−H), 7.67−7.68 (m, 2H, BT−H), 7.91 (d, 2H,, Ar−H), 7.98 (dd, 1H, BT−H). ^{13}C NMR ($CDCl_3$): 114.5, 120.5, 126.4, 127.4 129.4, 129.6, 134.1, 136.4, 136.7, 137.7, 153.4, 155.6. GC-MS (EI): *m*/*z* 238.

Synthesis of 4-Bromo-7-(4-methoxy-phenyl)-2,1,3-benzothiadiazole. 4,7-Dibromo-2,1,3-benzothiadiazole (1.56 g, 5.3 mmol), 4-methoxyphenyl boronic acid (0.81 g, 5.3 mmol), and [Pd(PPh_3)$_4$] (0.30 g, 10 mol %) were dissolved in toluene (25 mL) and THF (25 mL). A solution of 2 M Na_2CO_3 (4 mL) was added, and the reaction mixture was vigorously stirred while being refluxed at 85 °C for 20 h. The reaction mixture was poured in iced water (150 mL), and this aqueous mixture was extracted with ethyl acetate (3 × 250 mL). The combined organic extracts were dried ($MgSO_4$), filtered, and evaporated to dryness. The crude product were purified by column chromatography (5% ethyl acetate: PETH$_{40-60}$), followed by recrystalliztion from ethyl acetate to give the product as yellow needles (0.99 g, 58%). ^{1}H NMR ($CDCl_3$, δ): 3.88 (s, 3H), 7.05 (d, 2H), 7.52 (d, 1H), 7.83−7.91 (m, 3H). ^{13}C NMR ($CDCl_3$): 55.4, 112.2, 114.2, 127.3, 129.0, 130.4, 132.3, 133.6, 153.2, 153.8, 160.0. MS (EI) *m*/*z* 322 [M]$^+$. HRMS calcd for $C_{13}H_9BrN_2OS$, 319.9619; found, 319.9614.

Synthesis of 4-(4-Methoxyphenyl)-7-*p*-tolyl-2,1,3-benzothiadiazole (6a). 4-Bromo-7-(4-methoxyphenyl)-2,1,3-benzothiadiazole (1.51 g, 4.6 mmol), *p*-tolyl boronic acid (0.77 g, 5.7 mmol), and [Pd(PPh_3)$_4$] (0.27 g, 10 mol %) were dissolved in toluene (15 mL) and THF (15 mL). A solution of 2 M Na_2CO_3 (10 mL) was added, and the reaction mixture was vigorously stirred while being heating at reflux at 85 °C for 24 h. The reaction mixture was poured in ice water (150 mL) and extracted with ethyl acetate (3 × 250 mL). The combined organic extracts were dried ($MgSO_4$), filtered, and evaporated to dryness. The crude product was purified by column chromatography (5% ethyl acetate: PETH$_{40-60}$), followed by recrystallization from DCM/PETH$_{40-60}$ to give the product as yellow needles (0.32 g, 70%). ^{1}H NMR ($CDCl_3$, δ): 2.45 (s, 3H, ArCH_3), 3.90 (s, 3H, OCH_3), 7.09 (d, 2H), 7.35 (d, 2H), 7.74 (d, 2H), 7.84−7.96 (m, 4H). ^{13}C NMR ($CDCl_3$): 21.3, 55.4, 114.1, 127.3, 127.8, 129.1, 129.3, 129.2, 130.4, 132.7, 132.7, 134.6, 138.2, 154.2, 154.3, 159.8. MS (EI) *m*/*z* 332 [M]$^+$. HRMS calcd for $C_{20}H_{16}N_2OS$, 332.0983; found, 332.0974.

Synthesis of 4-(4-Methoxyphenyl)-7-(5-methylthiophen-2-yl)-2,1,3-benzothiadiazole (6b) and 4-(5′-Hexyl-2,2′-bithiophen-5-yl)-7-(4-methoxyphenyl)-2,1,3-benzothiadiazole (6c). Intermediates **6b** and **6c** were prepared similar to **6a** from 4-bromo-7-(4-methoxyphenyl)-2,1,3-benzothiadiazole and the respective boronic acid pinacol esters.

Characterization of 6b. Yellow needles. ^{1}H NMR ($CDCl_3$, δ): 2.60 (s, 3H, TpCH_3), 3.90 (s, 3H, OCH_3), 6.87 (d, 1H), 7.08 (d, 2H), 7.66 (d, 1H), 7.84 (d, 1H), 7.92 (m, 3H).

Characterization of 6c. Red solid. ^{1}H NMR ($CDCl_3$, δ): 0.91 (t, 3H), 1.27−1.45 (m, 6H), 1.71 (m, 2H), 2.83 (t, 2H, TpCH_2), 3.91 (s, 3H, OCH_3), 6.73 (d, 1H), 7.08 (d, 2H), 7.11 (d, 1H), 7.20 (d, 1H), 7.68 (d, 1H), 7.89 (d, 1H), 7.93 (d, 2H), 8.04 (d, 1H).

Synthesis of 4-(7-*p*-Tolyl-2,1,3-benzothiadiazol-4-yl)phenol (7a). To a suspension of **6a** (0.72 g, 2.2 mmol) in HBr (48%, 20 mL) was added hexadecyldibutylphosphonium bromide (0.14 g, 0.22 mmol), and the reaction mixture was stirred at 130 °C for 20 h. The mixture was cooled to room temperature, poured in iced water (150 mL), and extracted with diethyl ether (3 × 250 mL). The combined organic extracts were dried ($MgSO_4$), filtered, and evaporated to dryness. The crude product was purified through a short silica gel plug (DCM) eluting with 2% ethyl acetate/PETH$_{40-60}$, followed by recrystallization from DCM/PETH$_{40-60}$ to give the product as yellow needles (0.64 g, 94%). ^{1}H NMR ($CDCl_3$, δ): 2.44 (s, 3H), 7.05 (d, 2H), 7.33 (d, 2H), 7.71−7.88 (m, 4H). ^{13}C NMR ($CDCl_3$): 115.6, 127.4, 127.8, 129.1, 129.3, 130.2, 130.6, 132.6, 132.8, 134.6, 138.2, 154.1, 154.2, 155.8. MS (EI): *m*/*z* 318 [M]$^+$. HRMS calcd for $C_{19}H_{14}N_2OS$, 318.0827; found, 318.0823.

Synthesis of 4-(7-(5-Methylthiophen-2-yl)-2,1,3-benzothiadiazol-4-yl)phenol (7b) and 4-(7-(5′-Hexyl-2,2′-bithiophen-5-yl)-2,1,3-benzothiadiazol-4-yl)phenol (7c). Intermediates **7b** and **7c** were prepared similar to **7a** from **6b** and **6c**, respectively.

Characterization of 7b. Yellow powder. ^{1}H NMR ($CDCl_3$, δ): 2.44 (br,1H, OH), 2.58 (s, 3H, TpCH_3), 6.87 (d, 1H), 7.01 (d, 2H), 7.65 (d, 1H), 7.83 (d, 1H), 7.87 (d, 2H), 7.91 (d, 1H).

Characterization of 7c. Red powder. ^{1}H NMR ($CDCl_3$, δ): 0.91 (t, 3H), 1.27−1.45 (m, 6H), 1.71 (m, 2H), 2.83 (t, 2H, TpCH_2), 4.99 (br, 1H, OH), 6.74 (d, 1H), 7.01 (d, 2H), 7.12 (d, 1H), 7.20 (d, 1H), 7.68 (d, 1H), 7.86−7.91 (m, 3H), 8.04 (d, 1H).

Synthesis of 4-*p*-Tolyl-7-[4-(4-vinyl-benzyloxy)-phenyl]-2,1,3-benzothiadiazole (8a). To a solution of **7a** (0.60 g, 1.9 mmol) in dry acetonitrile (10 mL) and dry DMF (4 mL) was added 4-vinylbenzyl chloride (0.32 mL, 2.3 mmoL), followed by anhydrous K_2CO_3 (1.29 g, 9.4 mmol). The reaction mixture was stirred vigorously at 65 °C for 4 h, cooled to room temperature, poured in ice water (150 mL), and extracted with DCM (3 × 250 mL). The combined organic extracts were dried ($MgSO_4$), filtered, and evaporated to dryness. The crude product was purified by column chromatography starting with a 5% ethyl acetate/PETH$_{40-60}$ and eluting the product with 20% MeOH/ethyl acetate. The monomer is obtained as a bright-yellow powder (0.79 g, 96%). ^{1}H NMR ($CDCl_3$, δ): 5.27 (d, 1H), 5.77 (d, 1H), 6.73 (dd, 1H), 7.14 (d, 2H), 7.35 (d, 2H), 7.45 (s, 4H), 7.73 (d, 2H), 7.85 (d, 2H), 7.93 (d, 2H). ^{13}C NMR ($CDCl_3$) 154.1, 154.2, 159.0, 114.1, 115.0, 126.4, 127.7, 127.6, 127.8, 129.0, 129.3, 130.2, 130.4, 132.6, 132.8, 134.6, 136.4, 137.4, 138.2. HRMS (EI) calcd for $C_{28}H_{22}N_2OS$, 434.1453; found, 434.1446,.

Synthesis of 4-(5-Methylthiophen-2-yl)-7-(4-(4-vinylbenzyloxy)phenyl)-2,1,3-benzothiadiazole (8b) and 4-(5′-Hexyl-2,2′-bithiophen-5-yl)-7-(4-(4-vinylbenzyloxy)phenyl)-2,1,3-benzothiadiazole (8c). Monomers **8b** and **8c** were prepared similarly to **8a** from **7b** and **7c**, respectively, by stirring at room temperature overnight.

Characterization of 8b. Yellow powder after purification by column chromatography (hexane/$CHCl_3$ 1:1 v/v). Red needles suitable for XRD analysis obtained by slow diffusion of hexane in DCM. ^{1}H NMR ($CDCl_3$, δ): 2.58 (s, 3H, TpCH_3), 5.15 (s, 2H), 5.27 (d, 1H), 5.77 (d, 1H), 6.74 (dd, 1H), 6.87 (d, 1H), 7.14 (d, 2H), 7.43 (m, 4H), 7.65 (d, 1H), 7.83 (d, 1H), 7.89−7.93 (m, 3H). Data from single-crystal XRD analysis are shown in the Supporting Information.

Characterization of 8c. Red powder. ^{1}H NMR ($CDCl_3$, δ): 0.91 (t, 3H), 1.29−1.44 (m, 6H), 1.71 (m, 2H), 2.83 (t, 2H, TpCH_2), 5.15 (s, 2H), 5.27 (d, 1H), 5.78 (d, 1H), 6.73 (d, 1H), 6.74 (dd, 1H), 7.11 (d, 1H), 7.13 (d, 2H), 7.19 (d, 1H), 7.44 (m, 4H), 7.66 (d, 1H), 7.88 (d, 1H), 7.92 (d, 2H), 8.03 (d, 1H).

General Procedure for Free Radical Polymerization of Vinyl Monomers. A mixture of the radical initiator, monomer, and solvent was degassed with three freeze−pump−thaw cycles, sealed under vacuum, and heated in a constant-temperature oil bath for the stated time. The mixtures were then cooled and precipitated twice in MeOH, filtered, and washed with MeOH to give the polymers.

Characterization of P4. Yellow powder. ^{1}H NMR ($CDCl_3$, δ): 1.27, 2.38, 6.71, 7.5−7.9 (broad).

Characterization of P8a. Yellow powder. ^{1}H NMR (CDCl$_3$, δ): 0.91, 1.32, 1.72, 2.08, 2.40, 4.95, 6.71, 6.95, 7.20, 7.5−8.0.

Characterization of P8b. Orange powder. ^{1}H NMR (CDCl$_3$, δ): 1.44, 2.40, 4.77, 6.66, 7.14, 7.54, 7.6−8.0 (broad).

General Procedure for RAFT-Controlled Free Radical Polymerization of Vinyl Monomers. Mixtures of the 2-cyanopropan-2-yl butyl trithiocarbonate (RAFT agent), radical initiator, monomer, and solvent were degassed with three freeze−pump−thaw cycles, sealed under vacuum, and heated in a constant-temperature oil bath for the stated time. The polymers were precipitated twice into MeOH, filtered, and washed with MeOH.

Characterization of P2-RAFT. Light-yellow powder. ^{1}H NMR (CDCl$_3$, δ): 0.89, 0.99, 1.28, 1.79, 1.97, 2.18, 3.21, 6.08, 6.82.

Characterization of P8b-RAFT. Orange powder. ^{1}H NMR (CDCl$_3$, δ): 0.93, 1.15, 1.35, 1.57, 1.73, 2.07, 2.54, 3.27, 4.97, 6.97, 7.30, 7.46, 7.71, 7.93.

Characterization of P2-*b*-8b-RAFT. Orange powder. ^{1}H NMR (CDCl$_3$, δ): 0.92, 0.99, 1.31, 1.57, 1.78, 1.99, 2.19, 2.50, 3.23, 4.87, 6.08, 7.30, 7.45, 7.71, 7.93.

Characterization of P8c-RAFT. Red powder. ^{1}H NMR (CDCl$_3$, δ): 0.92, 1.34, 1.62, 2.18, 2.79, 6.0−8.25 (very broad).

Characterization of P2-b-8c-RAFT. Red powder. ^{1}H NMR (CDCl$_3$, δ): 0.92, 1.35, 1.65, 2.16, 2.79, 6.06, 6.78, 7.23, 7.51.

General Procedure for Removal of Thiocarbonylthio Group. The thiocarbonylthio groups were removed by radical-induced reduction using *N*-ethylpiperidine hypophosphite.[15] A typical procedure is described below.

A mixture of polymer **P8b-RAFT** (M_n = 11 230, M_w/M_n = 1.24, 280 mg, 0.022 mmol), *N*-ethylpiperidine hypophosphite (77 mg, 0.43 mmol), and Vazo-88 (5.3 mg, 0.022 mmol) in chlorobenzene (3.5 mL) was placed in an ampule, degassed with three freeze−pump−thaw cycles, sealed under vacuum, and heated to 110 °C for 4 h. The solution was precipitated in 80 mL of acetone, washed twice with 50 mL of acetone, and dried under vacuum. To ensure the complete removal of the thiocarbonylthio group, the polymer was afterward dissolved in 15 mL of CHCl$_3$ and 0.5 mL of *n*-butylamine and stirred overnight at room temperature. Removal of the solvent under reduced pressure gave a yellow polymer (265 mg, M_n = 13 050; M_w/M_n = 1.34).

Results and Discussion

Monomer Synthesis. To prepare functional polymers by radical polymerization, it is necessary to synthesize unsymmetrical electroactive pendant monomers. The design and synthesis is outlined in Scheme 1. As a hole-transporting pendant, we chose a triarylamine derivative, which is readily prepared by the palladium-catalyzed Buchwald−Hartwig cross coupling of di-*p*-tolylamine and 3-bromostyrene.[16] The methyl substituents in the para position have been chosen to prevent the known irreversible oxidative coupling of triphenylamine moieties.[17] The meta-substituted vinyl bond has been selected over its para-substituted isomer to break the symmetry and thus to give better solubility in the resulting polymer chain. Another reason is the known improved stability of the meta-linkage when used as hole-transporting material in OLEDs.[18]

BT is a well-known electron-deficient synthon utilized in small molecular dyes and fully conjugated polymers.[19] Thanks to its low-lying LUMO, it imparts electron-transporting properties to the resulting electroactive material. The first monomer prepared in this series was 4-vinyl-2,1,3-benzothiadiazole (Scheme S1 of the Supporting Information), which spontaneously polymerized when isolated to give low-molecular-weight oligomers. Given the instability of this monomer, no further attempts were made to resynthesize this compound.

Scheme 1. Synthesis of Benzothiadiazole- and Triarylamine-Containing Monomers

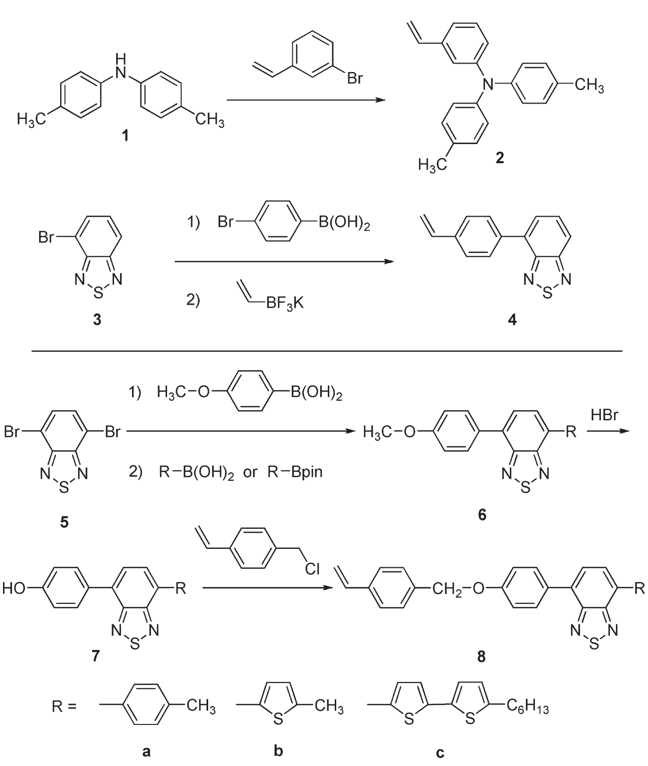

To obtain more stable monomers, the vinyl group was separated by a phenyl group in the second monomer 4-(4′-vinylphenyl)-2,1,3-benzothiadiazole (**4**), which was initially prepared from 4-vinylphenyl boronic acid. However, purification of the product was problematic because of the instability of the compound to the extensive chromatography necessitated by the presence of the byproduct 4,4′-divinyl-biphenyl. Monomer **4** was therefore obtained by reacting 4-(4-bromophenyl)-2,1,3-benzothiadiazole with potassium vinyltrifluoroborate.[13] This reaction is an efficient way of introducing the vinyl functionality and proceeded smoothly on a 1 g scale in 95% yield.

We prepared another three BT-containing monomers by isolating the electroactive pendants from their polymerizable styrene functionality. For this, we sandwiched the BT moiety between a methoxyphenyl on one side and a tolyl, a thiophenyl, and a bithiophenyl chromophore on the other side. Those electron-donating groups are expected to push electrons to the electron-withdrawing BT moiety forming donor−acceptor dyes **6a−c** with low band gaps.[20] The syntheses of the monomers were completed by deprotection of the methoxy-functionality with hydrogen bromide, followed by coupling with 4-vinylbenzyl chloride.

As part of the final purification procedure before polymerization, monomers were usually recrystallized. Slow diffusion of hexane into a concentrated dichloromethane solution formed large needle-like red crystals of monomer **8b**, which were suitable for X-ray diffraction (XRD) analysis. Molecular diagrams of the crystal structure from its top and side view are shown in Figure 1A,B, respectively. The structure of the BT pendant is very flat, with only the phenyl moiety slightly out of plane, suggesting a very good π-conjugation between the three aromatic rings. In contrast, the vinylbenzyl group is twisted in the opposite direction to the phenyl group, indicating only limited interaction between the two aromatic systems due to the nonconjugated −CH$_2$O spacer. The molecular packing of the monomers occurs along the *b* axis in an alternating up−down−up−down fashion of the BT chromophore, with each second monomer rotated 180°. The overlapping parts of each chromophore are always a BT with a thiophene ring with a distance between two units of 3.4 Å. This suggests a very tight packing and strong intermolecular interactions.

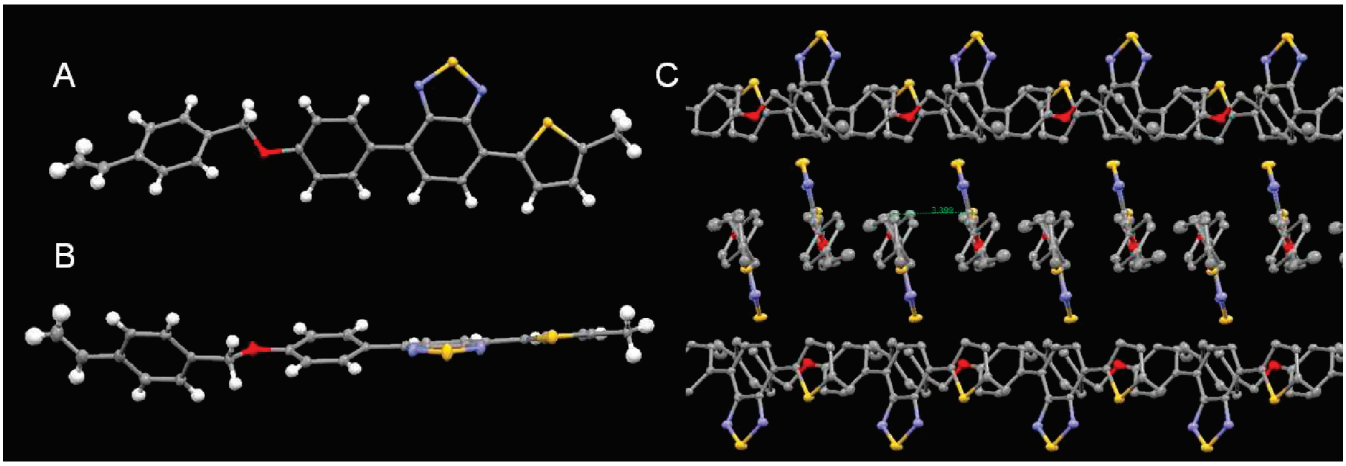

Figure 1. Molecular diagram of monomer **8b** shown with 50% thermal ellipsoids and hydrogen atoms as spheres of arbitrary size in (A) top view and (B) side view. (C) Molecular packing arrangement (hydrogen atoms are omitted for clarity).

Scheme 2. Synthesis of Electroactive Homo and Block Copolymers

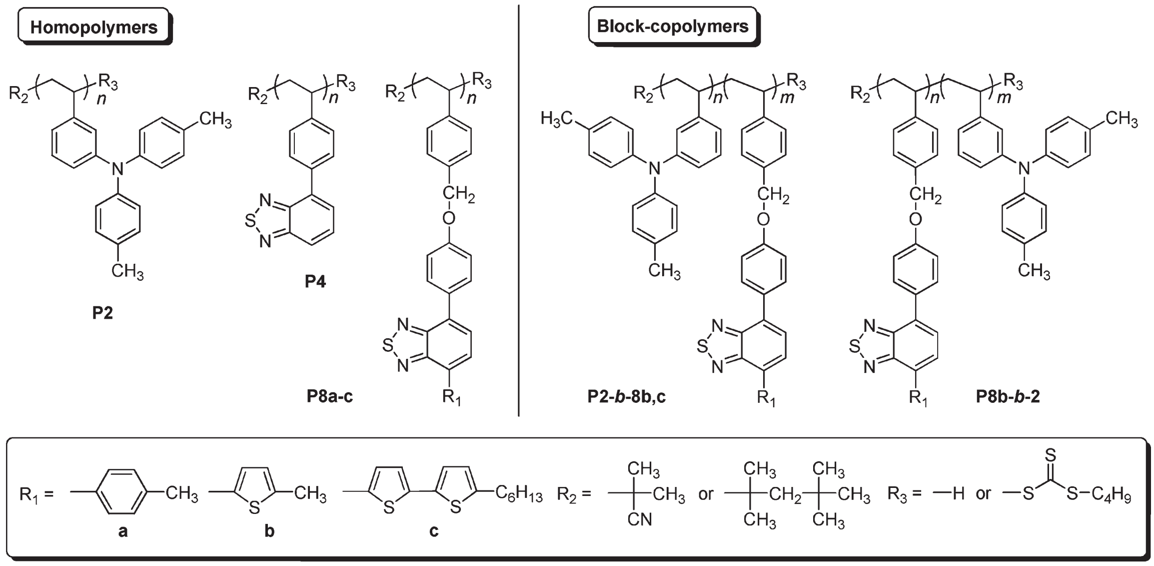

Polymerization. Homopolymers of the electroactive pendant monomers **2**, **4**, **8a**, and **8b** (Scheme 1) were obtained by free-radical polymerization in excellent yields (up to 95% conversion, Scheme 2 and Table 1). The MWs varied according to the monomer polymerized ranging from 7 to ~100 kDa. This broad variation can be attributed to variations in the solubility of the monomer and hence the molar concentration of the vinyl bonds. Monomer **2** and **8b** showed the highest solubility among the four monomers; therefore, less solvent was used for the polymerization, and as a result, the highest MWs were obtained. Attempts to increase the concentration of the monomers were only of limited success, and the data shown here represent the best results achieved to date. PS control polymerizations, carried out under comparable monomer concentrations, confirmed the obtained conversions and MWs. Monomer **8c** was available only in small quantities and only used during the following described controlled radical polymerizations.

To obtain well-defined block copolymers, monomers **2**, **8b**, and **8c** (Scheme 1) were selected to be polymerized under the control of a trithiocarbonate RAFT agent. These monomers were chosen on the basis of their potential electroactive properties because triarylamine is known as a hole-transporting material[16−18] and **8b** and **8c** are strongly colored (absorbing light in the visible region). All polymerizations proceeded smoothly, and polymers with expected MWs and very narrow MW distributions (M_w/M_n = 1.10 to 1.24) were obtained. From each of the macro-RAFT agents, a second block could be polymerized with slightly broader MW distribution in the range of 1.29 to 1.64, as demonstrated by the block copolymers **P2-*b*-8b**, **P2-*b*-8c**, and **P8b-*b*-2**.

In one of our previous studies, we found that the thiocarbonylthio group can interfere with the luminescence properties of the electroactive polymers and quench emitted light.[8a,21] We thus removed the thiocarbonylthio groups of the polymers investigated in the Optical Properties section of this article. We achieved removal of the thiocarbonylthio groups by reacting the final polymer with *N*-ethylpiperidine hypophosphite and AIBN, followed by treatment with *n*-butylamine. (See the Experimental Section for details.)[15]

Structural and Thermal Analysis. All polymers were characterized by spectroscopic methods, from which satisfactory analysis data corresponding to their molecular structures were obtained. (See the Experimental Section for details.) Figure 2 shows the ^{1}H NMR spectra of monomer **8b** and its RAFT-synthesized homopolymer **P8b-RAFT**. Whereas **8b** exhibits the characteristic resonance peaks of the vinyl group from the styrene moiety between 5.3 and 6.8 ppm, those

Table 1. Molecular and Thermal Properties of Homo and Block Copolymers[a]

	polymer	conv. (%)[b]	DP	$M_{n,\mathrm{theor}}$ (Da)[c]	M_n (Da)[d]	M_w (Da)[d]	M_w/M_n	T_g (°C)[e]	T_d (°C)[f]
1	**P2**	95.0			48 000	97 440	2.03	134	399
2	**P2-RAFT**	71.0	35	10 700	6180	7110	1.15	119	388
3	**P4**[g]	79			5990	11 720	1.96	150	400
4	**P8a**[h]	80			4730	7570	1.60	117	
5	**P8b**	80			21 860	34 990	1.60	130	353
6	**P8b-RAFT**	59.1	29	12 920	11 230	13 930	1.24	127	326
7	**P8b-RAFT**[g]	27.9	28	12 550	10 100	11 800	1.17	128	339
8	**P8c-RAFT**	52.0	26	15 620	13 420	15 400	1.15	122	
9	**P2-*b*-8b-RAFT**	78.9[i]	35/39	28 060	31 860	52 130	1.64	133	333
10	**P2-*b*-8c-RAFT**	68.5[i]	35/34	30 980	34 540	44 600	1.29	117	404
11	**P8b-*b*-2-RAFT**	64.4[i]	28/32	22 120	10 490	13 960	1.33	127	339
12	**P8b-*b*-2-RAFT**	39.0[i]	28/195	70 860	36 540	51 730	1.42	134	349

[a] Polymerization conditions: AIBN, chlorobenzene, 70 °C, 16 h, for RAFT polymerizations: [monomer]/[RAFT]/[initiator] 50:1:0.1. [b] Conversion. [c] The number-average molecular weight was calculated according to: $M_{n,\mathrm{theor}} = \mathrm{DP} \times M_{\mathrm{mono}} + M_{\mathrm{RAFT}} + M_{\mathrm{ini}}$, where DP is the degree of polymerization (obtained from ^{1}H NMR), M_{mono} is the molecular weight of the monomer, M_{RAFT} is the molecular weight of the RAFT agent, and M_{ini} is the molecular weight of the initiator fragment. [d] Molecular weight obtained from gel permeation chromatography in chloroform against polystyrene calibration. [e] Glass-transition temperature obtained from DSC at a heating rate of 10 °C/min under nitrogen. [f] Decomposition temperature obtained from TGA at a heating rate of 20 °C/min under nitrogen. [g] Initiator Vazo88 at 90 °C for 20 h, toluene. [h] Initiator V110 at 110 °C for 20 h, solvent: chlorobenzene/toluene 4:1. [i] Conversion of second block.

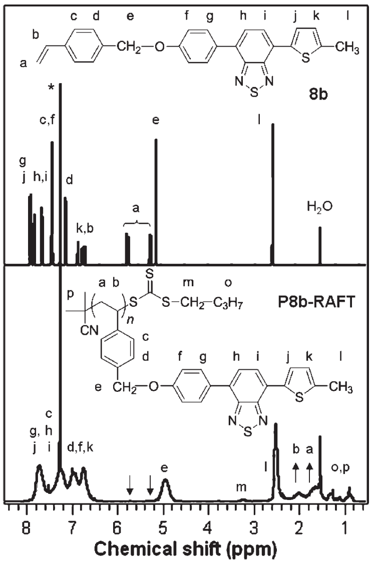

Figure 2. ^{1}H NMR spectra of monomer **8b** and its homopolymer **P8b-RAFT** (solvent is marked with asterisk).

peaks completely disappear after the polymerization. At the same time, new peaks emerge around 1.5 to 2.2 ppm associated with the formation of the PS polymer backbone.[22] Additionally, peaks at 0.8 to 1.4 and 3.2 ppm can be identified corresponding to the presence of the RAFT end group of the polymer chain. All other peaks are readily assigned to the electroactive pendant, confirming the proposed molecular structure.

The thermal properties of the polymers were evaluated using DSC and TGA, and the results are summarized in Table 1. Despite their large aromatic chromophores, which could potentially induce $\pi-\pi$ stacking and thus some higher order, all polymers are amorphous in nature (also confirmed by powder XRD shown in Figure S2 in the Supporting Information), and no transition peaks, such as melting points, were observed in the heating scan of the DSC. The glass-transition temperatures (T_g) of the pendant polymers are in the range of 120−150 °C, which is considerably higher than their atactic PS congener (T_g of ~100 °C).[23] As expected, the T_g of the homopolymers depends on the molecular structure and follows the trend **P8a** < **P8c** < **P8b** < **P2** < **P4**. This order is not very surprising because **P2** and **P4** should have the most rigid backbone due to their bulky ditolyl amine and BT groups, respectively, directly attached to the PS backbone and the lack of long solubilizing alkyl groups. It is somewhat surprising that **P8a** has a lower T_g than **P8c** because the latter polymer contains long hexyl groups in each repeating unit. It is likely that the presence of the two thiophene moieties in **P8c** (vs only a phenyl ring in **P8a**) negates the lubricating effects of the alkyl group. At the same time, the MW is known to influence the T_g as well, and it is usual for the T_g to increase with increasing MW.[24] This can be shown by comparing the low-molecular-weight **P2-RAFT** (M_n = 6180; T_g = 119 °C) with its structurally identical high-molecular-weight analog **P2** (M_n = 48 000; T_g = 134 °C).

The block copolymers show thermal properties similar to those of their homopolymer analogs, although only one T_g can be detected from DSC instead of two. This can be understood considering that the T_g values of all employed building blocks are in the same range of 127−134 °C. The only exception is **P2-*b*-8c-RAFT**, which exhibits a T_g of 117 °C, suggesting that the **P8c** block has a bigger influence on the thermal properties than the polytriarylamine block of **P2**.

TGA analysis shows all the pendant polymers to be very stable, with weight loss beginning at temperatures well above 300 °C (Table 1). Figure 3 illustrates the thermogram of polymer **P2** as an example. The triarylamine pendant polymer exhibits a constant weight until its final degradation temperature of ~400 °C. Its RAFT-synthesized analog **P2-RAFT** shows a slightly different behavior by losing around 3% of its original weight at ~230 °C. The weight afterward remains constant until ~390 °C before it reaches its final degradation temperature as well. The weight loss of the RAFT polymer can be rationalized by a concerted thermolysis of the trithiocarbonate end group.[25] As depicted in the inset of Figure 3, it is postulated that the high temperatures induce a 2 + 2 + 2 electron rearrangement resulting in an unsaturated polytriarylamine chain end plus *S*-butyl trithiocarboxylic acid, which readily decomposes into carbon disulfide and butyl thiol. The measured ~3% weight loss agrees very well with the amount of RAFT agent in **P2-RAFT**. Considering a measured MW of 6180 g/mol, the fragment of the RAFT agent weighs 165 g/mol, and this corresponds to 2.67 wt % in the polymer.

Optical Properties. One aim of this investigation was to study the optical properties of nonconjugated polymers with electroactive pendant. In contrast with conventional conjugated polymers, the electro-optical properties of the monomer are reflected in the resulting polymer because the polymerization does not alter the attached chromophoric unit. This is clearly illustrated in Figure 4. Chloroform solutions

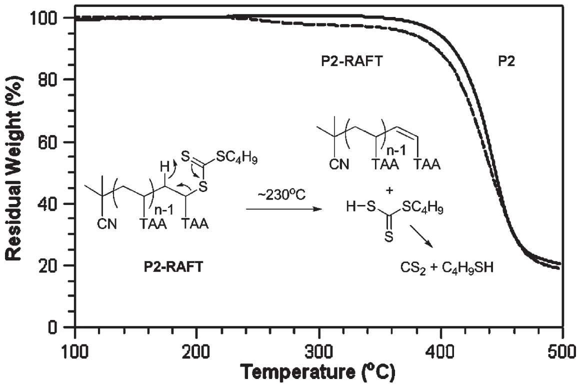

Figure 3. Thermal gravimetric analysis of **P2** and **P2-RAFT**. Inset shows proposed concerted mechanism for thermolysis of RAFT end groups occurring at ~230 °C (TAA = triarylamine fragment of **P2-RAFT**).

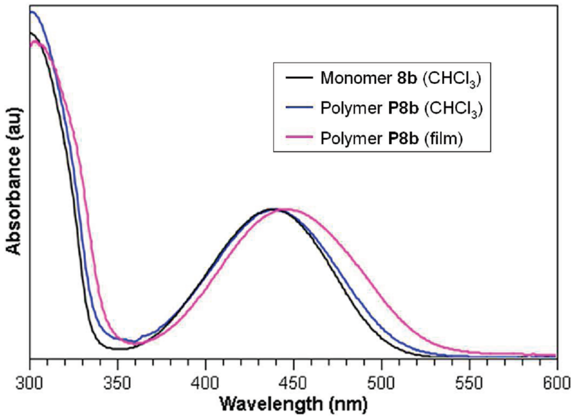

Figure 4. Normalized absorption spectra of monomer **8b** and its homopolymer **P8b** in chloroform solutions and as a thin film spin-casted from $CHCl_3$ solution.

of monomer **8b** and its homopolymer **P8b** show almost identical UV absorption peaks with their maximum at 440 nm. Even the solid state does not alter the absorption spectrum much, and only a 6 nm bathochromic shift can be observed when polymer **P8b** is spin-casted on a glass slide. All polymers are strongly absorbing in the visible region with molar extinction coefficients up to 35 000 M^{-1} cm^{-1} (cf. Figure S3 and S4 in the Supporting Information).

The retention of the absorption properties of the monomer chromophore in the polymer allows for a molecular engineering approach to variation of the electronic properties of the corresponding polymers. BT is known to be a strong, electron-withdrawing building block, and the attachment of an electron donor at its four- and seven-positions alters the bandgap of the resulting chromophore. This is demonstrated by variations in the UV absorption spectra of the four BT-containing homopolymers. As shown in Figure 5 and Table 2, the absorption band shifts to lower energy, an indication of increasing π-conjugation and increasing donor strength, as the number of aryl rings on the electroactive pendant increases. **P4**, with its BT moiety directly attached to the styrene backbone and only a proton as substituent at the seven-position, has the smallest conjugation path length and consequently exhibits the shortest absorption peak among all four polymers, peaking at 360 nm in dilute chloroform solution. The BT unit of polymers **P8a**, **P8b**, and **P8c** is sandwiched between an oxyphenyl on one side and a tolyl, thienyl, and bithienyl group, respectively, on the other. Substituting the proton of **P4** with a tolyl group in **P8a** extends the π-conjugation and red-shifts the maximum absorption by 45 nm. Although the conjugation path length of **P8b** is similar to that of **P8a**, the electron-rich thienyl group is a stronger donor than tolyl and as a consequence shows an even further bathochromic-shifted UV absorption with its maximum at 440 nm. Polymer **P8c** exhibits the largest π-conjugation among the four different pendants and as a result shows the longest wavelength absorption peak at 465 nm. Clearly, the UV absorption of the polymers is strongly affected by the choice of the pendant chromophore.

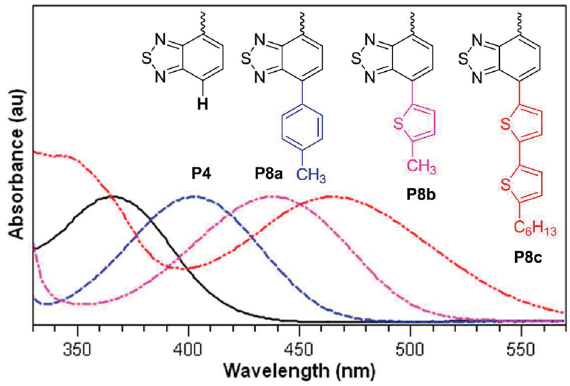

Figure 5. Normalized absorption spectra of benzothiadiazole-containing polymers in chloroform solutions.

The block copolymers also show similar absorption spectra compared with their homopolymer components with an additional peak at 305 nm from the triarylamine block (Table 2).

We continued our spectroscopic study by evaluating the photoluminescence properties of thin films of pendant homo and block copolymers. All homopolymers are highly fluorescent and emit light depending on their pendant chromophore in the broad range from 424 to 658 nm (Table 2).

The block copolymers show a somewhat different picture. Exciting block copolymer **P2-*b*-8b** at 350 nm, a wavelength that mainly excites the **P2** block as **P8b** exhibits an absorption minimum (cf. Figure 4), results in an emission peak at 585 nm originating from the **P8b** block (Figure 6). The emission peak of the polytriarylamine block **P2** at 424 nm is completely quenched. Such behavior suggests efficient interaction between the different electroactive pendants mainly in the form of energy transfer. More detailed photophysical investigations are currently underway to understand the electronic interactions between these two building blocks better.

Another interesting finding can be observed by exciting homopolymer **P8b** and its block copolymer **P2-*b*-P8** at 450 nm, a wavelength outside the polytriarylamine absorption. Despite having comparable UV absorptions of the BT chromophore at the excitation wavelength, which means identical numbers of photons are absorbed in both films, the block copolymer shows a higher luminescence than its homopolymer counterpart. Initial fluorescence lifetime measurements support these findings (Figures S5 and S6 in the Supporting Information),[26] which suggests that the BT chromophore undergoes self-quenching due to aggregate formation. These aggregates get broken up in the copolymer by the polytriarylamine blocks and as a result overcome the self-quenching.

Electronic Properties. To characterize fully our electroactive materials, we determined the HOMO and LUMO levels by cyclic voltammetry and PESA in combination with UV absorption and photoluminescence spectroscopy. Most of the BT-containing polymers **P4**−**P8** exhibit symmetrical, quasi-reversible oxidation and reduction peaks, from which

Table 2. Photophysical Properties of Thin Films of Homo and Block Copolymers

polymer	UV_{max} (nm)	PL_{max} (nm)	$E_{g,op}$ (eV)[a]	IP (eV)[b]	HOMO (eV)[c]	LUMO (eV)[c]	$E_{g,el}$ (eV)[d]
P2	305	424	3.40	−5.59	−5.25	n.d.	
P4	365	490	2.90	−5.70	−5.73	−2.85	2.88
P8a	415	541	2.59	−5.89	−5.42	−2.94	2.48
P8b	440	610	2.36	−5.85	−5.40	−2.99	2.41
P8c	467	658	2.20	−5.44	−5.27	−3.10	2.17
P2-*b*-8b	440	608	2.37	−5.60	−5.17	−2.99	2.18
P2-*b*-8c	468	651	2.22	−5.44	−5.25	−3.10	2.15

[a] Optical bandgap, determined by the onset of the UV absorption peak. [b] Ionization potential, measured from photoelectron spectroscopy in air (PESA). [c] HOMO and LUMO obtained from the onset of the peaks in the CV spectra against Fc/Fc$^+$ redox couple, assuming a HOMO level of ferrocene of −4.8 eV (n.d. = not detected). [d] Electronic bandgap, calculated from the differences between HOMO and LUMO level.

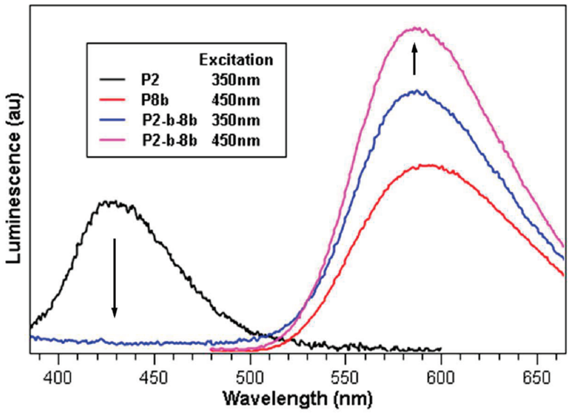

Figure 6. Photoluminescence spectra of thin films of pendant homo and block copolymers spun-coated on glass. The films were excited at 350 and 450 nm. The photoluminescence is normalized by the UV absorption of the films at the excitation wavelength.

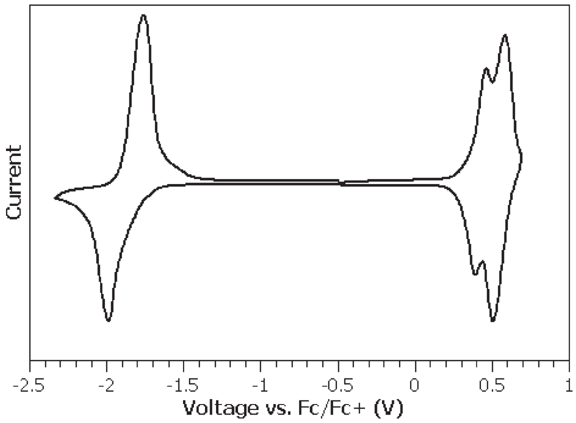

Figure 7. Cyclic voltammetry of **P2-*b*-P8b** spin-coated on the glassy carbon electrode.

HOMO and LUMO levels can be readily calculated using the ferrocenium/ferrocene redox couple as internal reference and assuming that this is related to the ferrocene HOMO level of −4.8 eV.[27] Figure 7 shows the cyclic voltammogram of **P2-*b*-P8b** spin-coated as thin film on top of a glassy carbon electrode. The plot shows two overlapping reversible oxidation peaks at 0.42 and 0.55 V, which, by comparison with CVs of the homopolymers, are assigned as originating from the triphenylamine and BT pendants, respectively. Additionally, a reversible reduction peak can be identified at −1.88 V associated with the BT unit as well. This suggests that the HOMO of **P2-*b*-P8b** is associated with the polytriarylamine block, whereas the LUMO is associated with the BT-containing pendant polymer block. This conclusion is supported by the measured IP of the block copolymer, which gives a value of −5.60 eV, very close to that of **P2** (−5.59 eV). The block copolymer **P2-*b*-8c** shows a slightly different behavior. Here both HOMOs and LUMOs are mainly associated with the BT-containing pendant polymer block, which is supported by the IP of −5.44 eV, similar to that of **P8c** (Table 2).

Film Morphology. A key parameter in device fabrication is the morphology of solid-state films. Rough or highly phase-segregated films are susceptible to electrical shorting, variation in current density, or both when used in devices. To study the effect of incorporating the electroactive groups into block copolymers on this key parameter, we prepared thin films of model compound **6b** and block copolymer **P2-*b*-P8b** as well as a blend of the two homopolymers **P2** and **P8b**. Model compound **6b** is similar to monomer **8b**, a highly crystalline material, and forms long needle-like crystals even when spin-coating films from $CHCl_3$ solution (Figure 8A). Blending two different polymers together usually results in a phase separation of the two materials. A similar behavior can be found by spin-casting solutions of homopolymers **P2** and **P8b** onto glass slides (Figure 8B). Very rough films are obtained with height differences up to 250 nm, suggesting the formation of phase-separated domains of homopolymers. In contrast, spin-casting solutions of block copolymer **P2-*b*-8b** gives very smooth films, demonstrating that block copolymers can be used to improve the morphology of films (Figure 8C).

Application in Organic Photovoltaic Devices. Thanks to their self-assembly behavior, donor−acceptor block copolymers could potentially be used as single component materials in bulk heterojunction solar cells. All attempts to utilize only our block copolymers in an OPV device, however, were unsuccessful, and no rectifying behavior was obtained. This can be rationalized by the fact that the block copolymers showed only limited self-quenching of their photoluminescence (cf. Figure 6), which translates into few charges being separated upon illumination.

To improve the electron transfer and to enhance the charge mobility in the devices, PCBM, a strong electron acceptor, was added. Figure 9a shows the dark and light current−voltage characteristics of a typical OPV device based on a **P2-*b*-8b**/PCBM 1:4 active layer composition. The strong rectification behavior in the dark highlights the favorable diode properties of the device. An equivalent circuit analysis of the diode suggests series and parallel resistance values of 6 Ω cm^2 and 750 kΩ cm^2, respectively. Although devices with varying ratios of **P2-*b*-8b**/PCBM were tested, the best devices were obtained from a blend ratio of **P2-*b*-8b**/PCBM of 1:4 with V_{oc}, J_{sc}, FF, and PCE of 0.77 V, 0.73 mA/cm^2, 0.28, and 0.16%, respectively. Whereas the V_{oc}, which reflects the difference between the ionization potential of the donor and the electron affinity of the acceptor, in this device is high, the photocurrent is relatively low. A comparison of the incident photon to current efficiency (IPCE) to the absorptance spectrum of the active film deposited on glass confirms that the photocurrent is

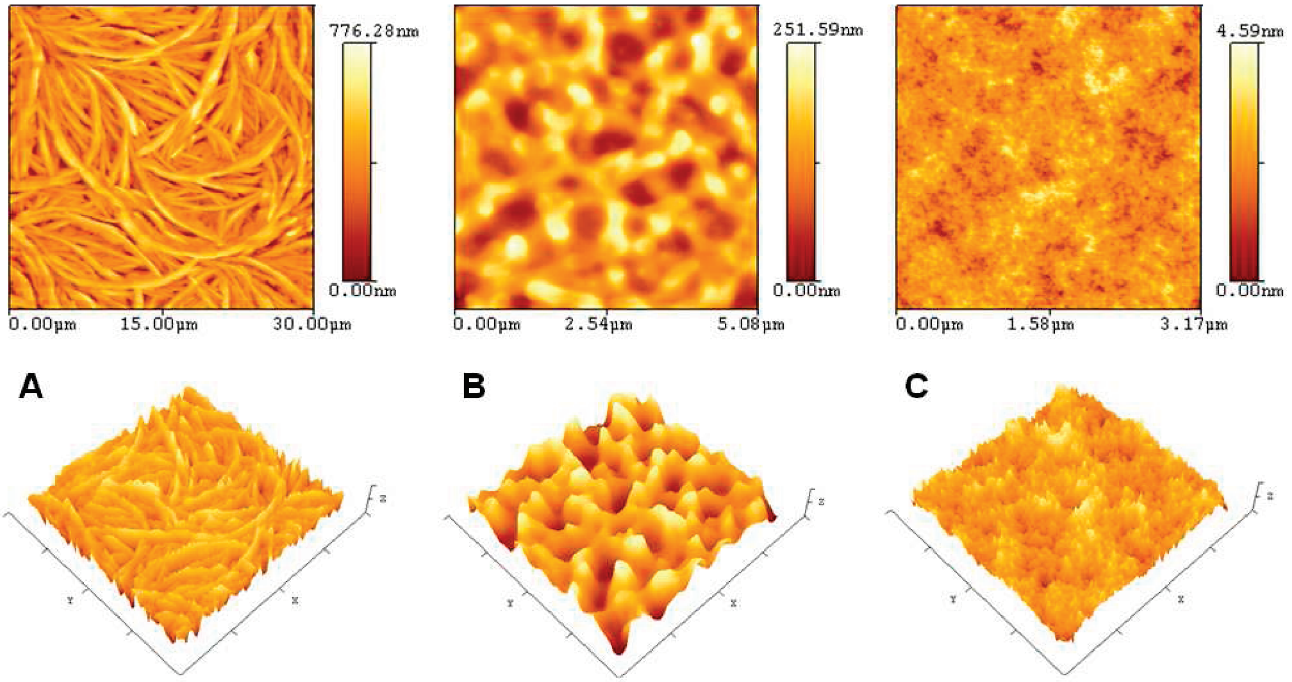

Figure 8. AFM images of thin films of (A) model compound **6b**, (B) blends of homopolymers **P2** and **P8b**, and (C) block copolymer **P2-*b*-P8b** spin-coated from 2 wt % $CHCl_3$-solutions.

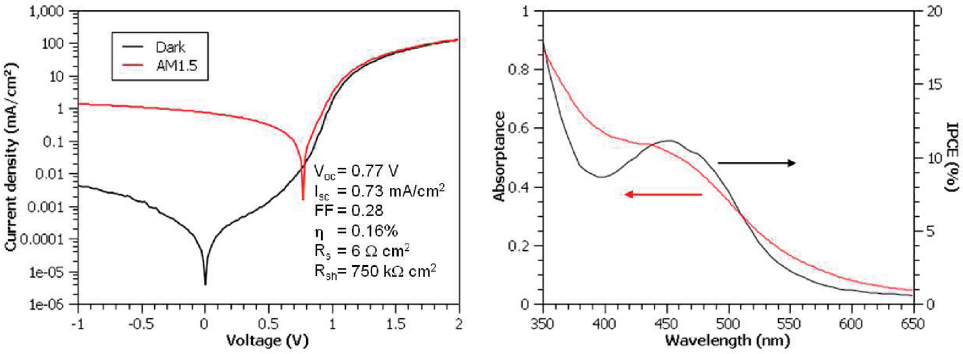

Figure 9. (A) Current−voltage curve of a 147 nm organic solar cell device consisting of a blend of block copolymer **P2-*b*-8b** and PCBM (blend ratio 1:4) as active layer. (B) IPCE and absorption spectra of active layer.

generated from the active layer (Figure 9b). Unfortunately, as indicated by the low FF, the excitons and carriers that are generated within this active layer are recombining strongly. Recent work on block copolymer systems suggests that their major benefits to OPV are as modifiers for morphology and as stabilizers of multicomponent mixtures.[28] Indeed, the use of our pendant polymers could be advantageously used in a similar manner.

Conclusions

New electroactive pendant polymers based on BT-containing chromophores have been synthesized by free radical polymerization with and without the control of a RAFT agent. RAFT synthesized polymers could be chain-extended to yield well-defined block copolymers. The resulting pendant homo- and block copolymers exhibit interesting photophysical properties such as efficient energy transfer between the chromophores. The block copolymers influenced the morphology of spin-casted films and showed rectifying behavior in OPV devices, making them potential candidates for various applications in the field of organic electronics.

Acknowledgment. This work was funded through the Flexible Electronics Theme of the CSIRO Future Manufacturing Flagship as part of an Office of the Chief Executive Postdoctoral Fellowship and was also supported by the Victorian Organic Solar Cells Consortium (Victorian Department of Primary Industries, Sustainable Energy Research and Development Grant) and the Australian Department of Innovation, Industry, Science and Research, International Science Linkage grant CG100059. We thank Prof. Andrew Holmes from the University of Melbourne for fruitful discussions and helpful suggestions.

Supporting Information Available: X-ray structural information on **8b**, powder XRD spectrum of **P8b**, absorption spectrum of **P8c**, single photon counting measurements, and an X-ray crystallographic file (CIF). This material is available free of charge via the Internet at http://pubs.acs.org.

Note Added after ASAP Publication. This article posted ASAP on August 6, 2010. The name of the seventh author of this paper has been changed from Saif A. Hague to Saif A. Haque. The correct version posted on August 17, 2010.

References and Notes

(1) (a) Cheng, Y. J.; Yang, S. H.; Hsu, C. S. *Chem. Rev.* **2009**, *109*, 5868. (b) Grimsdale, A. C.; Chan, K. L.; Martin, R. E.; Jokisz, P. G.; Holmes, A. B. *Chem. Rev.* **2009**, *109*, 897. (c) Bao, Z. Chapter 1. In *Polymers for Microelectronics and Nanoelectronics*; Lin, Q., Pearson, R. A., Hedrick, J. C., Eds.; ACS Symposium Series *874*; American Chemical Society: Washington, DC, 2004; pp 1−14. (d) Gunes, S.; Neugebauer, H.; Sariciftci, N. S. *Chem. Rev.* **2007**, *107*, 1324.

(2) (a) Peet, J.; Heeger, A. J.; Bazan, G. C. *Acc. Chem. Res.* **2009**, *42*, 1700. (b) Heremans, P.; Chenys, D.; Rand, B. P. *Acc. Chem. Res.* **2009**, *42*, 1740.

(3) (a) van Duren, J. K. J.; Yang, X. N.; Loos, J.; Bulle-Lieuwma, C. W. T.; Sieval, A. B.; Hummelen, J. C.; Janssen, R. A. J. *Adv. Funct. Mater.* **2004**, *14*, 425. (b) Babel, A.; Jenekhe, S. A. *Macromolecules* **2004**, *37*, 9835. (c) Sivula, K.; Ball, Z. T.; Watanabe, N.; Fréchet, J. M. J. *Adv. Mater.* **2006**, *18*, 206.

(4) (a) Bates, F. S.; Fredrickson, G. H. *Annu. Rev. Phys. Chem.* **1990**, *41*, 525. (b) Darling, S. B. *Prog. Polym. Sci.* **2007**, *32*, 1152. (c) Darling, S. B. *Energy Environ. Sci.* **2009**, *2*, 1266.

(5) Segalman, R. A.; McCulloch, B.; Kirmayer, S.; Urban, J. J. *Macromolecules* **2009**, *42*, 9205.

(6) (a) Moad, G.; Rizzardo, E.; Thang, S. H. *Aust. J. Chem.* **2005**, *58*, 379. (b) Moad, G.; Rizzardo, E.; Thang, S. H. *Aust. J. Chem.* **2006**, *59*, 669. (c) Moad, G.; Rizzardo, E.; Thang, S. H. *Aust. J. Chem.* **2009**, *62*, 1402.

(7) (a) Chen, M.; Ghiggino, K. P.; Mau, A. W. H.; Rizzardo, E.; Thang, S. H.; Wilson, G. J. *Chem. Commun.* **2002**, 2276. (b) Chen, M.; Ghiggino, K. P.; Thang, S. H.; Wilson, G. J. *Angew. Chem.* **2005**, *117*, 4442. (c) Chen, M.; Ghiggino, K. P.; Rizzardo, E.; Thang, S. H.; Wilson, G. J. *Chem. Commun.* **2008**, 1112.

(8) (a) Lindner, S. M.; Huttner, S.; Chiche, A.; Thelakkat, M.; Krausch, G. *Angew. Chem., Int. Ed.* **2006**, *45*, 3364. (b) Sommer, M.; Lindner, S. M.; Thelakkat, M. *Adv. Funct. Mater.* **2007**, *17*, 1493. (c) Tao, Y.; McCulloch, B.; Kim, S.; Segalman, R. A. *Soft Mater* **2009**, *5*, 4219.

(9) Bundgaard, E.; Krebs, F. C. *Sol. Energy Mater. Sol. Cells* **2007**, *91*, 954.

(10) (a) Marcus, R. A. *Annu. Rev. Phys. Chem.* **1964**, *15*, 155. (b) Karikomi, M.; Kitamura, C.; Tanaka, S.; Yamashita, Y. *J. Am. Chem. Soc.* **1995**, *11*, 6791.

(11) (a) Ozen, A. S.; Atilgan, C.; Sonmez, G. *J. Phys. Chem. C* **2007**, *111*, 16362. (b) van Mullekom, H. A. M.; Vekemans, J. A. J. M.; Meijer, E. W. *Chem.—Eur. J.* **1998**, *4*, 1235. (c) Peet, J.; Heeger, A. J.; Bazan, G. C. *Acc. Chem. Res.* **2009**, *42*, 1700. (d) Kitamura, C.; Tanaka, S.; Yamashita, Y. *Chem. Mater.* **1996**, *8*, 570.

(12) Pilgram, K.; Zupan, M.; Skiles, R. *J. Heterocycl. Chem.* **1970**, *7*, 629.

(13) Molander, G. A.; Rivero, M. R. *Org. Lett.* **2002**, *4*, 107.

(14) Chiefari, J.; Mayadunne, R. T. A.; Moad, C. L.; Moad, G.; Rizzardo, E.; Postma, A.; Skidmore, M. A.; Thang, S. H. *Macromolecules* **2003**, *36*, 2273.

(15) Chong, Y. K.; Moad, G.; Rizzardo, E.; Thang, S. H. *Macromolecules* **2007**, *40*, 4446.

(16) Hartwig, J. F. *Angew. Chem., Int. Ed.* **1998**, *37*, 2046.

(17) Seo, E. T; Nelson, R. F.; Fritsch, J. M.; Marcoux, L. S.; Leedy, D. W.; Adams, R. N. *J. Am. Chem. Soc.* **1966**, *88*, 3498.

(18) Deng, L.; Furuta, P. T.; Garon, S.; Li, J.; Kavulak, D.; Thompson, M. E.; Fréchet, J. M. J. *Chem. Mater.* **2006**, *18*, 386.

(19) (a) Kono, T.; Kumaki, D.; Nishida, J.; Sakanoue, T.; Motoyasu, K.; Tada, H.; Tokito, S.; Yamashita, Y. *Chem. Mater.* **2007**, *6*, 1218. (b) Zhang, M.; Tsao, H. N.; Pisula, W.; Yang, C. D.; Mishra, A. K.; Mullen, K. *J. Am. Chem. Soc.* **2007**, *12*, 3472. (c) Kitamura, C.; Tanaka, S.; Yamashita, Y. *Chem. Mater.* **1996**, *8*, 570.

(20) (a) Melucci, M.; Favaretto, L.; Bettini, C.; Gazzano, M.; Camaioni, N.; Maccagnani, P.; Ostoja, P.; Monari, M.; Barbarella, G. *Chem.—Eur. J.* **2007**, *13*, 10046. (b) Sonar, P.; Singh, S. P.; Sudhakar, S.; Dodabalapur, A.; Sellinger, A. *Chem. Mater.* **2008**, *20*, 3184. (c) Beaujuge, P. M.; Subbiah, J.; Choudhury, K. R.; Ellinger, S.; McCarley, T. D.; So, F.; Reynolds, J. R. *Chem. Mater.* **2010**, *22*, 2093.

(21) Chen, M.; Ghiggino, K. P.; Launikonis, A.; Mau, A. W. H.; Rizzardo, E.; Sasse, W. H. F.; Thang, S. H.; Wilson, G. J. *J. Mater. Chem.* **2003**, *13*, 2696.

(22) Brandolini, A. J.; Hills, D. D. *NMR Spectra of Polymers and Polymer Additives*; Marcel Dekker: New York, 2000.

(23) Rieger, J. *J. Therm. Anal.* **1996**, *46*, 965.

(24) Santangelo, P. G.; Roland, C. M. *Macromolecules* **1998**, *31*, 4581.

(25) Postma, A.; Davis, T. P.; Moad, G.; O'Shea, M. S. *Macromolecules* **2005**, *38*, 5371.

(26) Initial fluorescence lifetime measurements detect faster fluorescence decay for the homopolymer compared with the block copolymer. A detailed photophysical study to clarify this finding is underway and will be published in due course.

(27) D'Andrade, B. W.; Datta, S.; Forrest, S. R.; Djurovich, P.; Polikarpov, E.; Thompson, M. E. *Org. Electron.* **2005**, *6*, 11.

(28) (a) Kim, H. C.; Park, S. M.; Hinsberg, W. D. *Chem. Rev.* **2010**, *110*, 146. (b) Rajaram, S.; Armstrong, P. B.; Kim, B. J.; Frechet, J. M. J. *Chem. Mater.* **2009**, *21*, 1775.